Relationships between Static Mechanical Properties and SilviScan Measured Wood Properties in Loblolly Pine

Joseph Dahlen
Finto Antony
Laurence R. Schimleck
Richard F. Daniels

Abstract

Relationships between static bending modulus of elasticity (MOE) and SilviScan (SS) properties (SilviScan MOE [MOE_{SS}], specific gravity, and microfibril angle) were explored. Seventy-three clearwood specimens (25 by 25 by 406 mm) were cut from thirty-two 33-year-old loblolly pine trees. Relationships were calculated between MOE and MOE_{SS} ($R^2 = 0.77$); however, MOE_{SS}, calibrated using sonic resonance, averaged 25 percent higher than static MOE. Calibrating MOE_{SS} to static MOE instead of sonic resonance MOE resulted in similar prediction performance ($R^2 = 0.77$), but more importantly approximately equal prediction values. The results demonstrate the importance of properly utilizing SilviScan information for predicting loblolly pine properties in static bending.

Lumber grades are differentiated based on strength-reducing characteristics that affect wood mechanical properties such as modulus of elasticity (MOE) and modulus of rupture (MOR). The MOE is influenced by variation in density and microfibril angle (MFA; Megraw et al. 1999), while MOR is influenced by density, knots, and slope of grain (Kretschmann 2010). Wood properties including density and MFA vary significantly within tree, from pith to bark and stump to tip (Jordan et al. 2006, Antony et al. 2012), and lumber also varies significantly based on where it is cut from within a tree (Kretschmann and Bendtsen 1992).

Nondestructive tools and techniques have become popular because they allow for rapid characterization of wood properties (Ross 2015). During product manufacturing, nondestructive evaluation (NDE) is used to grade products such as lumber via evaluation of density or MOE (either static or dynamic; Carter et al. 2006, American Lumber Standards Committee 2014, Galligan et al. 2015, Ross 2015). Prior to manufacturing, NDE using acoustics can be used to segregate low MOE logs from a population (Carter et al. 2006). Prior to felling trees, the wood at breast height (1.37 m) can be evaluated by measuring the acoustic velocity determined via time-of-flight by positioning two transducers along the bole (Grabianowski et al. 2006, Wessels et al. 2011). The SilviScan suite of instruments has been widely utilized in research to measure and predict wood properties from pith-to-bark from 12-mm increment cores and wood disks. The information obtained from SilviScan can be used for a variety of purposes including in breeding programs to select families with superior wood and fiber properties, assess the impact of climate and silviculture on wood and fiber properties, and for linking wood and fiber properties to product properties. SilviScan estimates density via X-ray densitometry, MFA via X-ray diffractometry, and tracheid properties via automated microscopy and image analysis (Evans 1994, 2006). SilviScan predicts MOE_{SS} using a semiempirical model from density and X-ray

The authors are, respectively, Associate Professor and Former Research Scientist, Warnell School of Forestry and Natural Resources, Univ. of Georgia, Athens (jdahlen@uga.edu [corresponding author], fintoa@gmail.com); Professor, Dept. of Wood Sci. and Engineering, Oregon State Univ., Corvallis (Laurence.Schimleck@oregonstate.edu); and Professor Emeritus, Warnell School of Forestry and Natural Resources, Univ. of Georgia, Athens (ddaniels@uga.edu). This article was received for publication in July 2015. Article no. 15-00044.

Forest Prod. J. 68(1):37–42.
doi:10.13073/FPJ-D-15-00044

diffractometry signals (Evans 1994, 2006). Evans (2006) found material with low MOE had high MFA as well as higher background scattering, which is associated with a higher proportion of non-S_2 microfibrils compared with wood with high MOE. The α and β constants developed for the SilviScan MOE_{SS} equation are based on dynamic MOE calculated from density and acoustic velocity using the sonic resonance method (Evans 2006). The acoustic velocity is determined from the frequency of numerous acoustic pulses as follows:

$$\mathrm{AV} = 2f_0L \tag{1}$$

where AV is the weighted mean acoustic velocity (m s^{-1}), f_0 is the first harmonic frequency of an acoustic wave signal (Hz), and L is the length (m) of the material (Wang 2013). Dynamic MOE determined by acoustic velocity ($MOE_{dyn.AV}$) is calculated as

$$\mathrm{MOE_{dyn.AV}} = \rho(\mathrm{AV})^2 \tag{2}$$

where the unit for $MOE_{dyn.AV}$ is Pa, ρ is the density (kg m^{-3}), and AV is the acoustic velocity (m s^{-1}; Wang 2013).

While strong relationships have been reported between static and dynamic MOE, the dynamic values are often higher than the static values. Divós and Tanaka (2005), using clear spruce samples, observed a difference between dynamic MOE, measured using stress wave velocity and vibrations, and static MOE due to creep, with dynamic MOE being approximately 10 percent higher. For any nondestructive tool, it is important to determine how different the predicted values are with static properties. Ilic (2001) found strong relationships ($R^2 = 0.90$) between static bending and the sonic resonance method used by Evans (2006) for *Eucalyptus delegatensis*. SilviScan has been used to assess the wood properties of loblolly pine; however, the relationships between static bending properties and SilviScan measured wood properties and SilviScan predicted MOE are not known. Bawcombe (2012) recalibrated the SilviScan MOE predicted values to static values using Douglas-fir (*Pseudotsuga menziesii*) by changing the α parameter from 0.165 to 0.133, and this adjustment calibrated the SilviScan MOE to static properties. In this study, we examined the relationship between static MOE and MOR with SilviScan measured properties in loblolly pine trees (*Pinus taeda*). This information will improve the use of SilviScan as a tool to assess loblolly pine wood properties through the development of calibration models to relate SilviScan properties to static MOE and MOR.

Materials and Methods

Trees utilized in this study were sampled from a 33-year-old loblolly pine plantation at New Bern, North Carolina. At age 13, the plots in the study were thinned to 613 trees per hectare and then fertilized at age 14. Tree height averaged 26.1 m (standard deviation = 1.0 m), and diameter at breast height averaged 35.3 cm (standard deviation = 2.8 cm). Fifty-six 0.6-m bolts were collected at heights of 2.4, 7.3, and 12.2 m from the base of 32 trees; not all trees yielded three bolts (Fig. 1). The midpoints of the bolts were located at the specified height levels (2.4, 7.3, 12.2 m). A 38-mm radial slab was sawn at the pith from the bolts using a Wood-Mizer sawmill. The slabs were dried, jointed, and planed to 25 mm radial height. Seventy-three clear static bending samples with dimensions 25 by 25 by 406 mm (respectively, radial, tangential, and longitudinal dimensions) were prepared from the bolts. The static bending samples were cut from each bolt to correspond to wood produced following the fertilization treatment that occurred at age 14. Depending on the availability of clear wood, one or two samples per bolt were prepared. The samples were conditioned to 12 percent moisture content (MC) and tested in bending to determine MOE and MOR over a 355.6-mm span on a Tinius Olsen 5000, following ASTM D143 procedures (ASTM International 2014).

Following static bending testing, a 25 by 25 by 25-mm block was cut from each end. The blocks were cut from outside of the test span; no block had deformation from the static bending test. One block was used to determine the specific gravity, and the second block was used for SilviScan analysis. The specific gravity of the block was determined by oven-drying the sample and then adjusting the measured specific gravity to 7.7 percent MC (specific gravity [SG]) to correspond to the 7.7 percent MC associated with the SilviScan facility (40% relative humidity, temperature 20°C, that is roughly equivalent to 7.7% MC; Glass and Zelinka 2010). The MOE and MOR values were adjusted to 7.7 percent MC to correspond with the same conditions utilized by SilviScan facilities using the framework developed by Kretschmann and Green (1996) and implemented by Butler et al. (2016):

$$p_{\text{modeled}} = \Big(\mathrm{I} + a(\mathrm{MC}) + b(\mathrm{MC})^2 + c(\mathrm{SG}) + d(\mathrm{SG})^2 + e(\mathrm{MC})(\mathrm{SG})\Big) \times f \tag{3}$$

where p_{modeled} is modeled MOE or MOR, MC is the moisture content expressed as a percentage, SG is the specific gravity at ovendry weight and volume at 12 percent MC, I is 550 for MOE and 0.2134 for MOR, a is 102.0 for MOE and 0.63886 for MOR, b is –2.401 for MOE and –0.01469 for MOR, c is –517.1 for MOE and 23.092 for MOR, d is 5,710.5 for MOE and 26.384 for MOR, e is –148.6 for MOE and –1.642 for MOR, and f is the adjustment from pounds per square inch ($\times 10^3$) to GPa for MOE and MPa for MOR. The modeled property value at MC_X (p_{modeled}) was calculated and compared with the measured property at MC_X (p_{measured}), and then the calculated expected property at 7.7 percent MC was calculated ($p_{\text{modeled7.7\%}}$) and the measured property at MC_X was adjusted by

$$P_{\text{adjusted7.7\%}} = p_{\text{measured}} + \frac{p_{\text{measured}}}{p_{\text{modeled}}} \times (p_{\text{modeled7.7\%}} - p_{\text{modeled}}) \tag{4}$$

where $p_{\text{adjusted7.7\%}}$ is the moisture adjusted MOE and MOR, and p_{measured} is the measured MOE and MOR of the small clear specimen.

The second set of 25 by 25 by 25-mm blocks were sent to the Commonwealth Scientific and Industrial Research Organization, Forestry and Forest Products, Australia, where a radial strip, 2 by 7 by 25 mm (respectively, tangential, radial, and longitudinal dimensions), were cut from each block. Wood properties of the radial strips were measured using SilviScan (Evans 1994, 2006) in a controlled environment equivalent to 7.7 percent MC. SilviScan specific gravity (SG_{SS}) was estimated using X-ray densitometry, and MFA was estimated using scanning

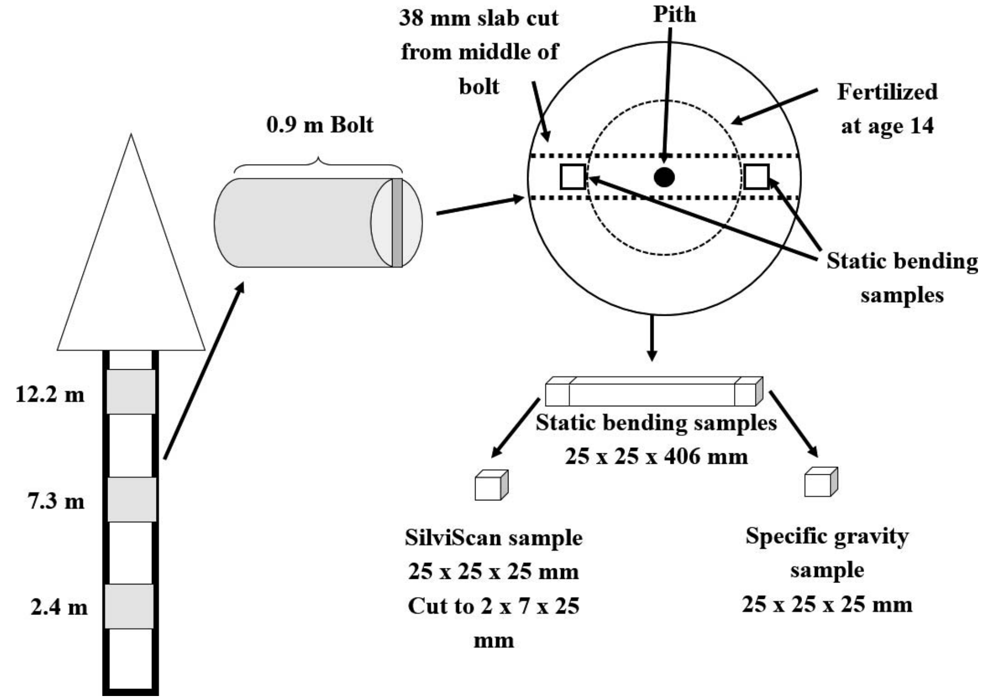

Figure 1.—Sampling schematic for the study whereby 0.9-m bolts were collected from three different heights within the trees (2.4, 7.3, and 12.2 m). Static bending samples were prepared from the bolts to correspond with wood produced following a fertilization treatment. Specific gravity and SilviScan samples were collected from the ends of the static bending samples.

X-ray diffractometry. SilviScan MOE (MOE_{SS}) was estimated by combining the information of SG_{SS} and I_{CV} (Evans 2006).

The SilviScan model was recalibrated from sonic resonance MOE to static bending MOE using the equation that SilviScan predicts MOE using density and the X-ray diffractometry signal:

$$MOE_{SS} = \alpha(I_{CV}\rho)^{\beta} \quad (5)$$

where I_{CV} is the coefficient of variation of the normalized azimuthal intensity, ρ is measured density in kilograms per cubic meter, and the α and β are constants (0.165 and 0.85) to account for scaling and curvature, which were calibrated from the sonic resonance calibration (Evans 1994, 2006). Using nonlinear least squares, different constants were evaluated for loblolly pine tested in static bending. Bawcombe (2012) reported for static bending using Douglas-fir that a value of $\alpha = 0.133$ results in a calibrated model instead of the 0.165 value for dynamic MOE. Here models were explored where the α and β parameters were allowed to vary, and then only one parameter was allowed to vary. Statistics were conducted using R 3.2.2 statistical software (R Core Team 2015) with RStudio (RStudio 2015). The plots were produced using the extrafont package (Winston 2014) for R. The nonlinear least squares (nls) function in R was used for recalibrating the SilviScan MOE equation.

Results and Discussion

The results from the study are summarized in Table 1 by sampled height. The mean MOE_{SS} is overestimated by 25, 28, and 22 percent at heights of 2.4, 7.3, and 12.2 m, respectively, and overall by 25 percent compared with mean MOE ($P < 0.0001$ at all heights; Fig. 2). The differences between MOE and MOE_{SS} become greater for samples with higher MOE. There was no consistent trend based on height. In addition to the differences in creep, some of the differences could be due to estimation error from SilviScan and the method SilviScan used to calculate MOE (Evans 2006, Verrill et al. 2011) and whether the SilviScan sample is representative of the parent material (Nakao et al. 1995), which in this case is a comparison between the 7-mm longitudinal SilviScan section with the 355.6-mm longitudinal small clear sample tested in between the reaction points of the static bending test. The Evans (2006) calibration model with SilviScan and sonic resonance had a strong but not perfect relationship ($R^2 = 0.94$) with a standard prediction error of 1 GPa. Verrill et al. (2011) raised concerns about SilviScan with regard to the variation of MFA, the accuracy of the X-ray intensity variation being a function of the MFA variability, and the effect that fiber tilt can have on the MFA prediction. Thus, as the fiber orientation tilts away from a longitudinal section, the accuracy of the measurement becomes a concern. Another difference may be due to the span-to-depth ratio. The 14:1 span-to-depth ratio used here is in accordance with ASTM D143 (ASTM International 2014); however, Sorn et al. (2011) in testing MOE from 3.4 to 30 span-to-depth ratios found that MOE decreases when ratios less than 20 are used. Sorn et al. (2011) recommended that MOE be measured at ratios greater than or equal to 20. These reasons help explain why SilviScan MOE is not perfectly correlated with static MOE measured here at 14 to 1 span-to-depth ratio. However, while they are different, MOE_{SS} and MOE are significantly correlated (Table 2), and a linear relationship explained 77 percent of variation in one given the other (Table 3).

Table 1.—Summary statistics of each wood property measured by sampled height.

Property[a]	2.4 m (n = 19)			7.3 m (n = 27)			12.2 m (n = 27)		
	Range	Mean	SD	Range	Mean	SD	Range	Mean	SD
MOE	7.7–14.2	11.3	2.0	6.4–11.2	8.5	1.2	4.9–9.7	6.8	1.0
MOE_{SS}	9.8–17.9	14.0	2.3	7.9–13.8	10.9	1.8	5.9–11.3	8.2	1.4
MOR	85.6–133.5	113.5	14.0	67.6–98.2	81.6	10.2	53.3–99.7	73.5	10.3
SG	0.53–0.66	0.59	0.04	0.38–0.53	0.45	0.04	0.35–0.47	0.41	0.03
SG_{SS}	0.54–0.65	0.59	0.03	0.38–0.51	0.45	0.04	0.35–0.47	0.41	0.03
MFA	11.1–24.4	16.8	3.8	12.1–20.5	16.0	2.4	13.9–28.1	19.1	2.8
$SG_{ss}MFA^{-1}$	25.3–50.5	36.7	7.6	19.8–39.7	28.8	5.3	14.9–31.6	21.8	4.2

[a] MOE = static modulus of elasticity (GPa); MOE_{SS} = SilviScan modulus of elasticity (GPa); MOR = modulus of rupture (MPa); SG = measured specific gravity; SG_{SS} = SilviScan SG; MFA = microfibril angle (°); $SG_{ss}MFA^{-1}$ = SilviScan specific gravity × MFA^{-1} × 1,000.

Using nonlinear least squares, we found a similar α parameter (α = 0.131) to Bawcombe (2012; α = 0.133), who found the value for static bending using Douglas-fir. Changing the α parameter from 0.165 to 0.131 resulted in a comparable model fit between the predicted values and the measured values (Fig. 2). The similar α parameter for static bending for two species mirrors the similar species results that Evans (2006) found for parameter estimation when calibrating *Eucalyptus delegatensis* and *Pinus radiata* (radiata pine) to sonic resonance MOE. The reduction in α from 0.165 for sonic resonance to 0.131 for static bending reduces the prediction value of MOE, which is comparable to the differences between static and dynamic MOE (Divós and Tanaka 2005).

The MOE and MOE_{SS} do have high correlations with specific gravity (SG and SG_{SS}), inverse of MFA (MFA^{-1}), and with the ratio between SG_{SS} and MFA (SG_{ss}/MFA; Table 2; Fig. 3). The strength of relationship between MOE and SG_{SS} ($R^2 = 0.68$) was observed to be higher than that with MFA^{-1} ($R^2 = 0.25$). However, the strength of the correlation between MOE_{SS} with SG_{SS} ($R^2 = 0.66$) and MFA^{-1} ($R^2 = 0.55$) was approximately equal. Similar results were reported by Lachenbruch et al. (2010) in static bending samples collected from >20-year-old Douglas-fir, where they observed a weaker correlation between MOE with MFA^{-1} ($R^2 = 0.22$) than with SG ($R^2 = 0.34$). However, Ivković et al. (2009) found slightly higher correlations between MFA and MOE ($R^2 = 0.31$) than between SG and MOE ($R^2 = 0.21$) in juvenile radiata pine. The MFA values ranged from 11.1° to 28.1° with a mean of 17.3° and standard deviation of 3.2°. These MFA values are typical of mature wood (Jordan et al. 2006). Via et al. (2009) found for longleaf pine that MFA explained more variation in MOE than in SG, whereas in mature wood they found that SG explained more variation in MOE than in MFA. These results align with the literature, which suggests that SG is a more important property for predicting MOE than is MFA in mature wood.

$SG_{ss}MFA^{-1}$ was well correlated with MOE, and their linear relationship explained 68 percent of variation for MOE. However, the linear relationship did not result in an improved model over SG_{SS} by itself ($R^2 = 0.68$). The differences in explained variation in MOE and MOE_{ss} ($R^2 = 0.77$) compared with $SG_{ss}MFA^{-1}$ reinforce the fact that there is not a linear relationship between MOE with SG and MFA and demonstrate the importance of the non-S_2

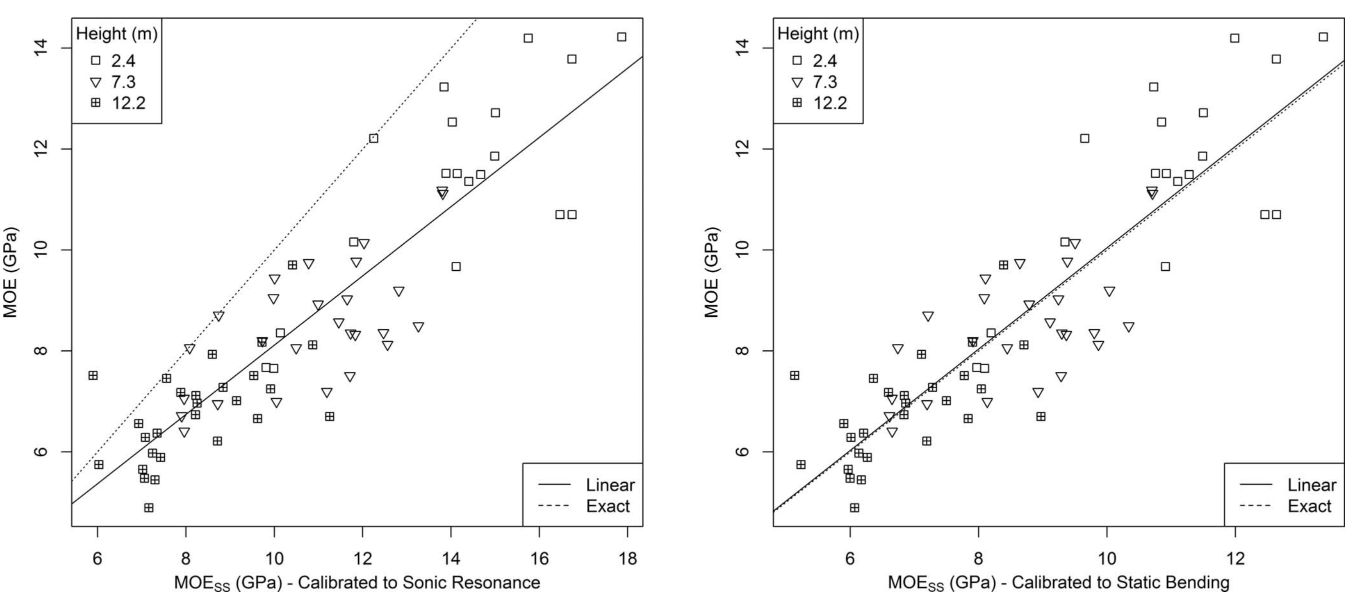

Figure 2.—Plot showing the static bending modulus of elasticity (MOE) and SilviScan predicted MOE (MOE_{SS}) as calibrated using sonic resonance (α = 0.165; left) and to loblolly pine static bending samples (α = 0.131; right). The solid diagonal line represents the linear regression fit, and the diagonal dashed line represents the line of equivalence ($R^2 = 0.77$).

Table 2.—Pearson correlation matrix among wood properties measured.[a]

Property	MOE_{SS}	MOR	SG	SG_{SS}	MFA^{-1}	$SG_{SS}MFA^{-1}$
MOE	0.88	0.87	0.85	0.82	0.51	0.83
MOE_{SS}		0.75	0.81	0.81	0.75	0.98
MOR			0.92	0.91	0.23	0.68
SG				0.97	0.29	0.75
SG_{SS}					0.26	0.75
MFA^{-1}						0.83

[a] MOE = static modulus of elasticity (GPa); MOE_{SS} = SilviScan modulus of elasticity (GPa); MOR = modulus of rupture (MPa); SG = measured specific gravity; SG_{SS} = SilviScan SG; MFA^{-1} = inverse of microfibril angle (°); $SG_{SS}MFA^{-1}$ = SilviScan specific gravity × MFA^{-1} × 1,000.

Table 3.—Estimated parameters and coefficients of determination from linear regression models.[a]

	Response								
	MOE			MOE_{SS}			MOR		
Predictor	Intercept	Slope	R^2	Intercept	Slope	R^2	Intercept	Slope	R^2
MOE				1.02	1.13	0.77	21.37	7.60	0.76
MOE_{SS}	1.25	0.69	0.77				32.03	5.11	0.56
MOR	−0.08	0.10	0.76	1.12	0.11	0.56			
SG	−2.70	23.92	0.71	−3.14	29.32	0.65	−21.07	228.11	0.85
SG_{SS}	−2.28	23.18	0.68	−3.05	29.30	0.66	−18.36	223.73	0.83
MFA^{-1}	2.43	103.60	0.26	−0.90	194.95	0.55	62.63	406.49	0.04
$SG_{SS}MFA^{-1}$	2.06	0.23	0.68	0.82	0.35	0.95	39.93	1.66	0.45

[a] MOE = static modulus of elasticity (GPa); MOE_{SS} = SilviScan modulus of elasticity (GPa); MOR = modulus of rupture (MPa); SG = measured specific gravity; SG_{SS} = SilviScan SG; MFA^{-1} = inverse of microfibril angle (°); $SG_{SS}MFA^{-1}$ = SilviScan specific gravity × MFA^{-1} × 1,000.

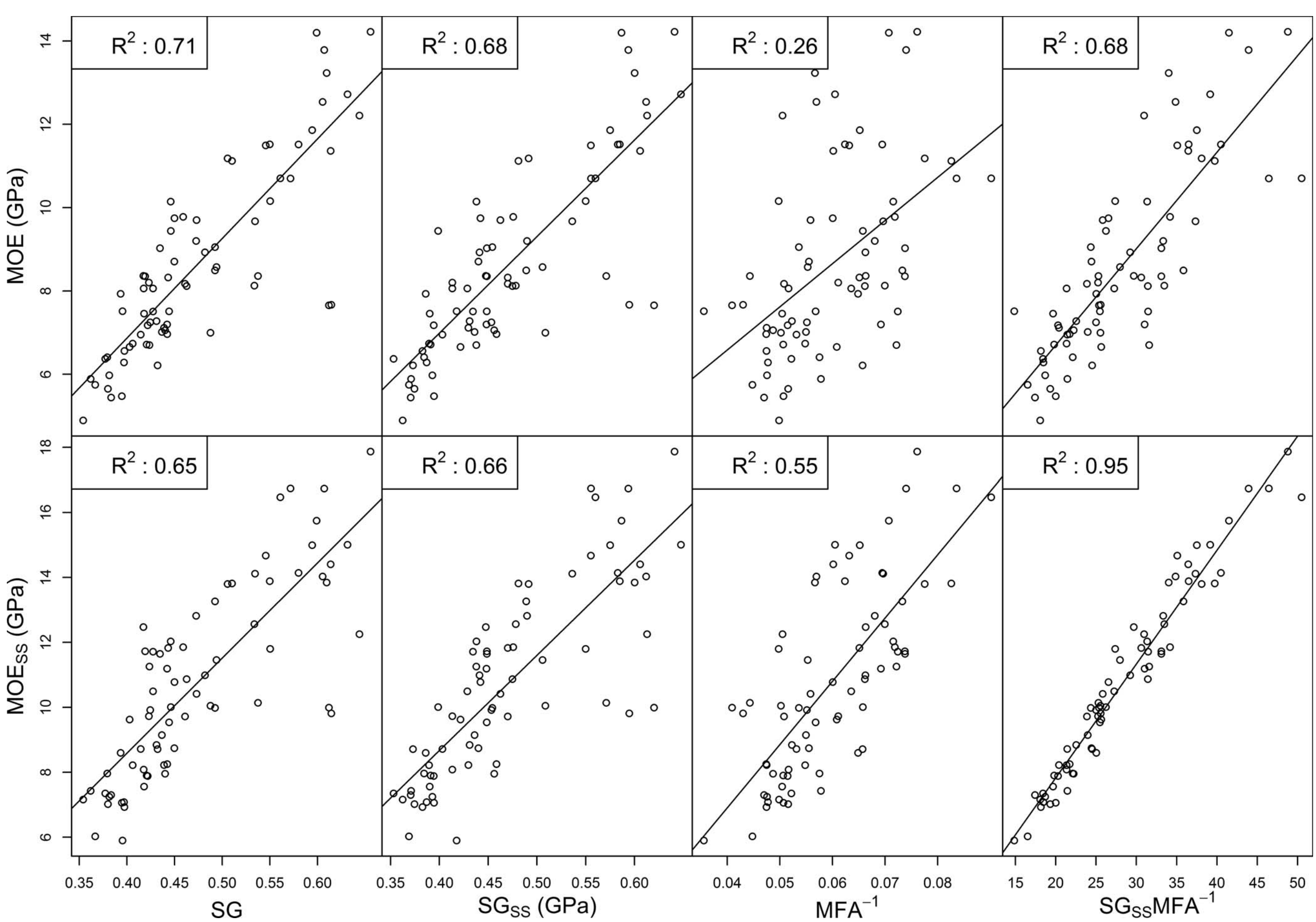

Figure 3.—Panel plot showing the relationship between static bending modulus of elasticity (MOE, top row) and SilviScan predicted MOE (MOE_{SS}, bottom row) with measured specific gravity (SG), SilviScan specific gravity (SG_{SS}), inverse of microfibril angle (MFA^{-1}), and Silviscan SG × MFA^{-1} × 1,000 ($SG_{SS}MFA^{-1}$), along with the linear regression lines.

microfibrils; these are accounted for in the I_{CV} measurement.

As expected, the direct measure of SG as determined on the small clear sample and the SilviScan measure of SG estimated from a block cut from the small clear sample were strongly correlated ($r = 0.97$). The Pearson correlation of MOR with SG ($r = 0.92$) and SG_{ss} ($r = 0.91$) was strong. The correlation between MOR and SG_{ss}/MFA was moderate, and their linear relationship explained only 45 percent of the variation in MOR.

Conclusions

A strong relationship was observed between MOE and MOE_{SS} ($R^2 = 0.77$); however, MOE_{ss} was on average 25 percent higher than MOE, and as the values increased, the differences between MOE_{ss} and MOE increased. Calibrating SilviScan MOE to static bending values instead of sonic resonance values resulted in MOE_{SS} being approximately equal to MOE. The calibrated α parameter found in this study for static bending ($\alpha = 0.131$) was less than the α parameter found for sonic resonance ($\alpha = 0.165$). The difference between dynamic MOE and static MOE should be considered and accounted for while estimating tree and wood properties for loblolly pine using nondestructive tools such as SilviScan.

Acknowledgment

The authors thank the Wood Quality Consortium and its partners for their support of this project.

Literature Cited

American Lumber Standards Committee (ALSC). 2014. Machine graded lumber policy. November 7, 2014. ALSC, Frederick, Maryland.

Antony, F., L. Schimleck, L. Jordan, R. Daniels, and A. Clark. 2012. Modeling the effect of initial planting density on within tree variation of stiffness in loblolly pine. *Ann. Forest Sci*. 69(5):641–650.

ASTM International. 2014. Standard test methods for small clear specimens of timber. ASTM D143. ASTM International, West Conshohocken, Pennsylvania.

Bawcombe, J. M. 2012. A study of Douglas-fir anatomical and mechanical properties and their interactions. PhD thesis. University of Bath, UK.

Butler, M. A., J. Dahlen, F. Antony, M. Kane, T. L. Eberhardt, H. Jin, K. Love-Myers, and J. P. McTague. 2016. Relationships between loblolly pine small clear specimens and dimension lumber tested in static bending. *Wood Fiber Sci*. 48(2):81–95.

Carter, P., S. Chauhan, and J. Walker. 2006. Sorting logs and lumber for stiffness using Director HM200. *Wood Fiber Sci*. 38(1):49–54.

Divós, F. and T. Tanaka. 2005. Relation between static and dynamic modulus of elasticity of wood. *Acta Silvatica Lignaria Hung*. 1:105–110.

Evans, R. 1994. Rapid measurement of the transverse dimensions of tracheids in radial wood sections from *Pinus radiata*. *Holzforschung* 48(2):168–172.

Evans, R. 2006. Wood stiffness by X-ray diffractometry. *In:* Characterization of the Cellulosic Cell Wall. D. D. Stokke and L. H. Groom (Eds.). Blackwell Publishing, Iowa State University Press, Ames. pp. 138–146.

Galligan, W., J. Kerns, and B. K. Brashaw. 2015. Machine grading of lumber. *In:* Nondestructive Evaluation of Wood. 2nd ed. R. J. Ross (Ed.). General Technical Report FPL-GTR-238. USDA Forest Service, Forest Products Laboratory, Madison, Wisconsin. 169 pp.

Glass, S. V. and S. L. Zelinka. 2010. Moisture relations and physical properties of wood. *In:* Wood Handbook. General Technical Report FPL-GTR-190. USDA Forest Service, Forest Products Laboratory, Madison, Wisconsin.

Grabianowski, M., B. Manley, and J. C. F. Walker. 2006. Acoustic measurements on standing trees, logs and green lumber. *Wood Sci. Technol*. 40(3):205–216.

Ilic, J. 2001. Relationships among the dynamic and static elastic properties of air-dry *Eucalyptus delegatensis* R. Baker. *Holz Roh-Werkst*. 59:169–175.

Ivković, M., W. J. Gapare, A. Abarquez, J. Ilic, M. W. Powell, and H. X. Wu. 2009. Prediction of wood stiffness, strength, and shrinkage in juvenile wood of radiata pine. *Wood Sci. Technol*. 43:237–257.

Jordan, L., R. Re, D. B. Hall, A. Clark III, and R. F. Daniels. 2006. Variation in loblolly pine cross-sectional microfibril angle with tree height and physiographic region. *Wood Fiber Sci*. 38(3):390–398.

Kretschmann, D. E. 2010. Stress grades and design properties for lumber, round timber, and ties. *In:* Wood Handbook—Wood as an Engineering Material. USDA Forest Service, Forest Products Laboratory, Madison, Wisconsin.

Kretschmann, D. E. and B. A. Bendtsen. 1992. Ultimate tensile stress and modulus of elasticity of fast-grown plantation loblolly pine lumber. *Wood Fiber Sci*. 24(2):189–203.

Kretschmann, D. E. and D. W. Green. 1996. Modeling moisture content-mechanical property relationships for clear southern pine. *Wood Fiber Sci*. 28(3):320–337.

Lachenbruch, B., G. R. Johnson, G. M. Downes, and R. Evans. 2010. Relationships of density, microfibril angle, and sound velocity with stiffness and strength in mature wood of Douglas-fir. *Can. J. Forest Res*. 40(1):55–64.

Megraw, R. A., D. Bremer, G. Leaf, and J. Roers. 1999. Stiffness in loblolly pine as a function of ring position and height, and its relationship to microfibril angle and specific gravity. *In:* Third Workshop-Connection between Silviculture and Wood Quality through Modeling Approaches. IUFRO, La Londeles Maures, France. pp. 341–349.

Nakao, T., C. Tanaka, A. Takahashi, and Y. Nishino. 1995. Experimental study of flexural vibration of wooden beams by Levison beam theory. *J. Vib. Acoust*. 117:378–379.

R Core Team. 2015. R 3.2.2: A language and environment for statistical computing. R Foundation for Statistical Computing, Vienna. http://www.R-project.org/.

Ross, R. J. 2015. Nondestructive testing and evaluation of wood. *In:* Nondestructive Evaluation of Wood. 2nd ed. USDA Forest Service, Forest Products Laboratory, Madison, Wisconsin.

RStudio. 2015. RStudio: Integrated development environment for R (Version 0.99.473). RStudio, Boston, Massachusetts.

Sorn, S., R. Bajramovic, and V. Hadziabdic. 2011. Examination of proper span/depth ratio range in measuring the bending strength of wood based on the elementary bending theory. 15th International Research/Expert Conference ''Trends in the Development of Machinery and Associated Technology'' TMT 2011, Prague, September 12–18, 2011, Czech Republic.

Verrill, S., D. E. Kretschmann, V. L. Herian, M. C. Wiemann, and H. A. Alden. 2011. Concerns about a variance approach to X-ray diffractometric estimation of microfibril angle in wood. *Wood Fiber Sci*. 43:153–168.

Via, B. K., C. L. So, T. F. Shupe, L. H. Groom, and J. Wikaira. 2009. Mechanical response of longleaf pine to variation in microfibril angle, chemistry associated wavelengths, density, and radial position. *Compos. Part A—Appl. Sci. Manuf*. 40:60–66.

Wang, X. 2013. Acoustic measurements on trees and logs: A review and analysis. *Wood Sci. Technol*. 47:965–975.

Wessels, C. B., F. S. Malan, and T. Rypstra. 2011. A review of measurement methods used on standing trees for the prediction of some mechanical properties of timber. *Eur. J. Forest Res*. 130:881–893.

Winston, C. 2014. Extrafont: Tools for using fonts. R package version 0.17. http://CRAN.R-project.org/package=extrafont.